Experimental characterization of a silicone oil-in-water droplet generator based on a micro T-junction

B Rostami, B Pulvirenti, G Puccetti and G L Morini

DIN – Alma Mater Studiorum Università di Bologna, Laboratorio di Microfluidica, Via del Lazzaretto 15/5, Bologna 40131, Italy

Corresponding Author Email: behnam.rostami2@unibo.it

Abstract. This paper deals with the emulsion of two immiscible fluids in a micro T-junction. An opposed-flow micro T-junction obtained by means of square microchannels (with a side of 300 μm) fabricated in a pure fused glass chip has been used for the formation of silicone oil-in-water (O/W) droplets. The experimental results have been obtained by considering both pure deionized water and a mixture of deionized water and surfactant (Tween 20) as the continuous flow. The results shown in this paper highlight that the presence of surfactant, also in very small concentrations, is able to change drastically the flow patterns of the two-phase flow generated by the T-junction. Concentration in weight of Tween 20 between 1 and 2% in the continuous flow is able to promote highly monodispersed emulsions with low polydispersity, especially for low flow rate ratios between the dispersed and continuous phase flows. On the contrary, by avoiding the use of surfactant, a stratified flow is obtained. The experimental results obtained in this work have been used in order to link the depth ratio of the stratified flow and the non-dimensional length of the plugs in droplet-based flow to the flow rate ratio between the dispersed and continuous flows.

1. Introduction

Micro T-junctions can be employed in order to obtain stable emulsions characterized by droplets with regular dimensions of the orders of tens/hundreds of microns. Microdroplets are now widely used in DNA and blood analysis [1], chemical reactions [2], food processing [3] and drug discovery [4]. Stable emulsions are characterized by droplets (dispersed or droplet forming phase) generated in the liquid core (continuous phase). The most studied emulsions in literature are those obtained by mixing water and oil; micro T-junctions and flow-focusing microdevices are the most preferred droplet generators due to their ease in fabrication and their capability to generate stable emulsions with droplet sizes easily controlled by means of the flow rates of the continuous and dispersed phase imposed at the inlet of the device. Thorsen *et al.* [5] were the first researchers who proposed the use of a T-junction into a microdevice for the generation of droplets [5, 6] as well as bubbles [7].

About the modelling of these devices, Garstecki *et al*. [8] observed that the squeezing mechanism is the main mechanism of the droplet formation and they proposed a simple physical model for the analysis of squeezing which is actually the basis of the developed correlations for these devices. Steegmans *et al*. [9] and Xu *et al*. [10] concentrated their attention on the physical mechanisms which control the droplet breakup. Guillot and Colin [11] and Tan *et al*. [12] focused their analysis on the influence of the continuous and dispersed phase flow rates on the control of the flow patterns

generated. Their conclusion is that the flow rate ratio α between the dispersed and continuous phase ($\alpha=Q_d/Q_c$) is the main responsible of the transition between different flow patterns.

Series of analysis have been focussed on the influence of the junction geometry on the characteristics of the two-phase flows; Das and Das [13], Raj *et al.* [14] and Steegmans *et al.* [15] studied the emulsion production by means of Y-junction by changing the angle between the inlet and main channel while Yeom and Lee [16] studied λ-junction. However, by observing the literature, the cross-flow and perpendicular T-junction geometries are the most studied configurations for the generation of emulsions [17]. The T-junction can be used under two operative configurations: the cross-flow and the opposed-flow configurations. Qian and Lawal [18] suggested using the opposed-flow configuration when gas bubbles are generated in a liquid continuous flow. Recently, Shui *et al*. [19] tested the opposed-flow configuration also for droplet generation by using both O/W and W/O droplets.

In this paper an experimental campaign focused on the analysis of the generation of stable silicone oil-in-water droplets in a T-junction under opposed-flow configuration is described. Firstly, the two-phase flow generated by means of a micro T-junction while no surfactant is added to the continuous phase is analyzed in a wide range of volumetric flow rates of oil (from 5 to 100 ml/h) and water (from 5 to 120 ml/h). Secondly, the effect of the presence of a small concentration of surfactant (=2 wt%) in the continuous phase is analyzed by observing the variation of the flow pattern due to the presence of the surfactant for each couple of volumetric flow rates (water from 1 to 25 and oil from 0.1 to 13 ml/h) imposed at the inlet of the T-junction.

2. Experimental apparatus

The experimental test rig shown in figure 1 is composed of an inverted microscope (1, *Nikon Eclipse TE2000-U*) with a double system of illumination obtained by means of a Mercury lamp (2a, *Nikon C-SHG1*) which is used to illuminate the T-junction from the bottom and a COB LED lamp (2b, *100W, 9000 Lumens*) which is able to illuminate the microdevice from the top. An air immersion lens with a numerical aperture *NA*=0.25 and magnification *M*=10x (3, *Nikon*, *CFI DS 10X*) is used to zoom the T-junction; a high-speed camera (4, *Olympus I-speed II*) is connected to the inverted microscope in order to be able to acquire a series of images with a maximum frame rate of 5000 fps. A LCD monitor (5) is used for a run-time visualization of the flow within the microdevice. In order to impose the silicone oil and the water volumetric flow rates at the inlet of the junction, two independent syringe pumps (6, *Harvard Apparatus PHD4400 Programmable* and 7, *Cole-Parmer Version Hills*) are employed.
By considering the declared accuracy of the syringe pumps, the uncertainty on the imposed volumetric flow rate Q_c and Q_d is equal to ±0.5% and ±0.35%, respectively.

A commercial micro T-junction (*Translume Co*.) has been chosen in this study; it is obtained by means of two perpendicular square microchannels having a side of 300 μm; the microchannels are microfabricated on a fused silica glass chip. The top surfaces of the microchannels are polished (optical polishing); on the contrary, the sidewalls and the bottom walls (translucent floor) of the channels are characterized by a random roughness of the order of 1 micron. The top surfaces show hydrophilic behaviour; on the contrary the other walls might be considered slightly hydrophobic.

All the square microchannels have the same width and depth, denoted as w_c, h_c for the continuous phase and w_d, h_d for the dispersed phase channel. The main characteristics useful to control the droplet generation within the T-junction are: the flow rate Q associated to the continuous (Q_c) and dispersed phase (Q_d), the main physical properties of the fluids involved (density ρ, dynamic viscosity μ) for both continuous and dispersed phase fluids and the interfacial tension σ between the liquids. The Buckingham-Pi theorem shows that the fluid dynamic behaviour of the T-junction is a function of the following dimensionless quantities: $\Lambda=w_d/w_c$, $L_c=h_c/w_c$, $L_d=h_d/w_d$, $\alpha=Q_d/Q_c$, $\lambda=\mu_d/\mu_c$, named width ratio, aspect ratio of the continuous and dispersed phase, flow rate ratio and viscosity ratio, respectively. The Capillary number ($Ca=Q\mu/\sigma wh$) and Reynolds number ($Re=\rho Q/\mu h$) associated to the dispersed and continuous phase. In this case, since the T-junction is made up of square microchannels, all the geometrical ratios Λ, L_c and L_d, are equal to unity.

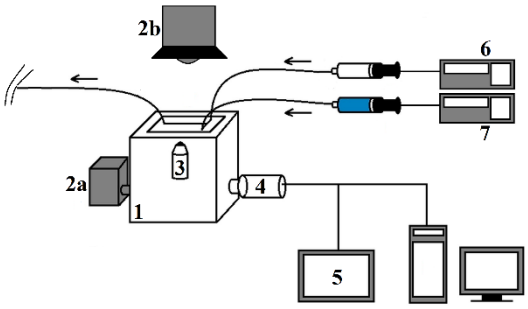

Figure 1. The experimental setup

The T-junction has been tested in this work under opposed-flow configuration. In figure 2a sketch of the T-junction with the indication of the position of the inlets of the dispersed and of the continuous phase is given: the continuous and dispersed phase meet at the junction head-to-head.

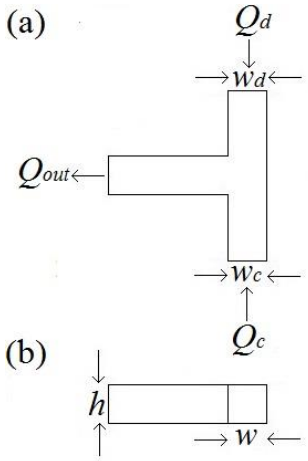

Figure 2. Sketch of the top (a) and side view (b) of the opposed-flow T-junction tested in this work

The silicone oil (Sigma Aldrich, viscosity 20 cSt, density 0.95 g/ml @ 25 °C) has been employed as the dispersed phase in the tests and the deionized water (viscosity 0.89 cSt, density 0.998 g/ml @ 25 °C) is considered as the continuous phase. Tween 20 (Sigma Aldrich, density 1.095 g/ml @ 25 °C) is used in a series of experimental tests as surfactant added to the deionized water in small concentrations (<2 wt%) in order to help the generation of stable oil-in-water emulsions (O/W droplets). Tween 20 (miscible in water) is a non-ionic detergent widely used in biochemical applications. The Hydrophilic-Lipophilic Balance (HLB) value of a surfactant is generally used to determine if the surfactant is hydrophobic or hydrophilic. Emulsifiers with high HLB values enhance the production of oil-in-water; on the contrary, surfactants with low HLB values give water-in-oil (W/O) emulsions [19]. Tween 20 is a hydrophilic surfactant having HLB=16.7 and it can be proficiently used for O/W emulsions.

3. Results

3.1. The effect of surfactant

Since the surface effects are dominant at microscale, small concentrations of surfactants added to the continuous phase can strongly enhance the droplet generation in microdevices as demonstrated by many papers [19, 20]. The surfactant adsorption in liquid-liquid systems acts dynamically in the droplet formation and strongly influences the values assumed by the interfacial tension σ. If σ is reduced, the mixing energy decreases and, as a consequence, the droplet generation becomes easier.

The presence of surfactant added to the continuous phase is more important when a T-junction under opposite-flow configuration is tested; in this configuration, in fact, the mixing tends to generate

stratified flow instead of droplets at the exit of the junction, so the presence of a surfactant can help to create stable emulsions, as demonstrated in [19].

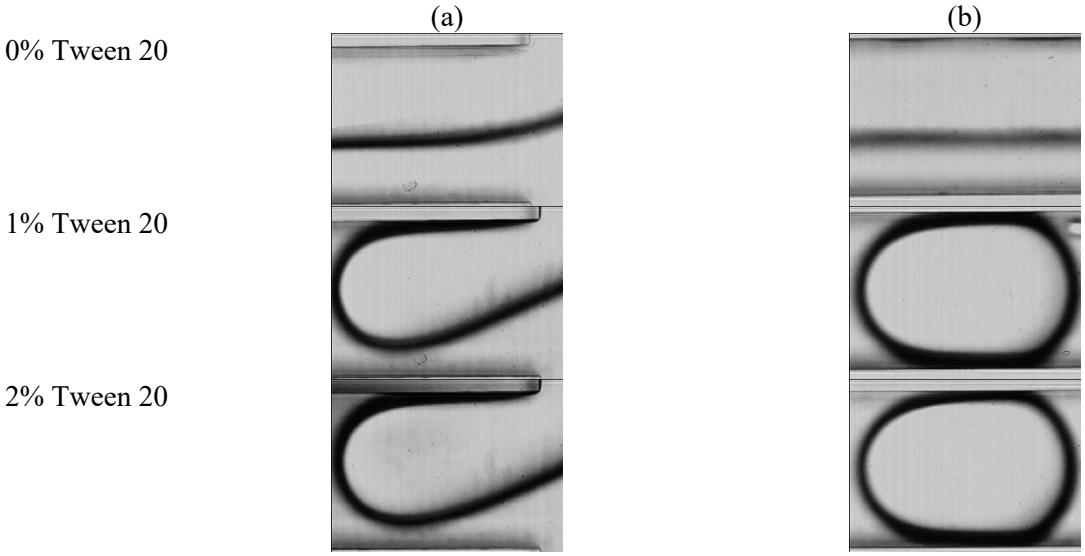

Figure 3. Interface geometry at the junction (a) and downstream (b) as a function of the concentration of Tween 20 added to the water when Q_c=25 ml/h and Q_d=5 ml/h (α=0.2)

Figure 3 shows the effect of Tween 20 on the silicone oil droplet formation in water. A volumetric flow rate of water equal to 25 ml/h has been imposed at the entrance (bottom-top direction in figure 3) against a volumetric flow rate of 5 ml/h of silicone oil (top-bottom direction in figure 3). The images are recorded by means of the speed camera and the evolution of the interface is reconstructed by means of a Matlab code using the Image Toolbox functions [21]. Without surfactant, the streams are not able to generate a droplet regime but they originate a stratified flow downstream of the junction.

Now, the same test has been repeated by adding Tween 20 to the water flow; since the critical micelle concentration (CMC), defined as the surfactant concentration above which micelles are spontaneously formed, of Tween 20 in water is equal to 0.0074% (w/v), values of concentration larger than 1% are more than sufficient in order to reduce to its minimum value the interfacial tension σ.

For this reason, two values of concentration of Tween 20 in water have been used during the tests: 1 wt% and 2 wt%. The largest value has been used in order to verify if the minimum value of the interfacial tension has been reached when the lowest concentration value is adopted.

By adding Tween 20 in water with a concentration of 1 wt%, the geometry of the interface at the junction drastically changes due to the reduction of σ; now, the largest flow rate of water (with respect to the silicone oil flow rate) is able to squeeze the silicone oil against the edge of the T-junction by generating the detachment of a regular oil droplet, as evidenced by the image taken downstream the T junction (figure 3b). In this condition a stable O/W emulsion is generated.

The results shown in figure 3 demonstrate that the increase of concentration between 1 to 2% is not able to produce any change on the geometry of the interface at the junction (which means the droplet formation mechanism is the same) and on the features of the oil droplets obtained downstream.

3.2. Water without surfactant

As evidenced by figure 3, without surfactant the flow regime after the T-junction is typically a stratified regime in which two parallel streams of silicone oil (on the top in figure 3) and water (on the bottom in figure 3) fill the cross section of the channel in laminar regime. Twenty three different experimental runs have been carried out by varying the inlet flow rates in a wide range from 5 up to 120 ml/h. For each value assumed by the flow rate ratio α^{-1} ($=Q_c/Q_d$), the ratio between the depth of the water (H_c) and the oil (H_d) streams has been calculated. For a fixed viscosity ratio (in this case

μ_c/μ_d=0.0467) and fixed geometry and flow configuration of the T-junction, the depth ratio H_c/H_d associated to the stratified flow, easily obtained by the image post-processing as shown in figure 4a, is a function of α. The uncertainty on H_c and H_d is linked to the thickness of the interface which depends on the illumination system. In this case the typical thickness of the interface is of the order of 14 pixels which corresponds to an uncertainty of 19 μm. The trend of the depth ratio as a function of flow rate ratio is shown in figure 4b.

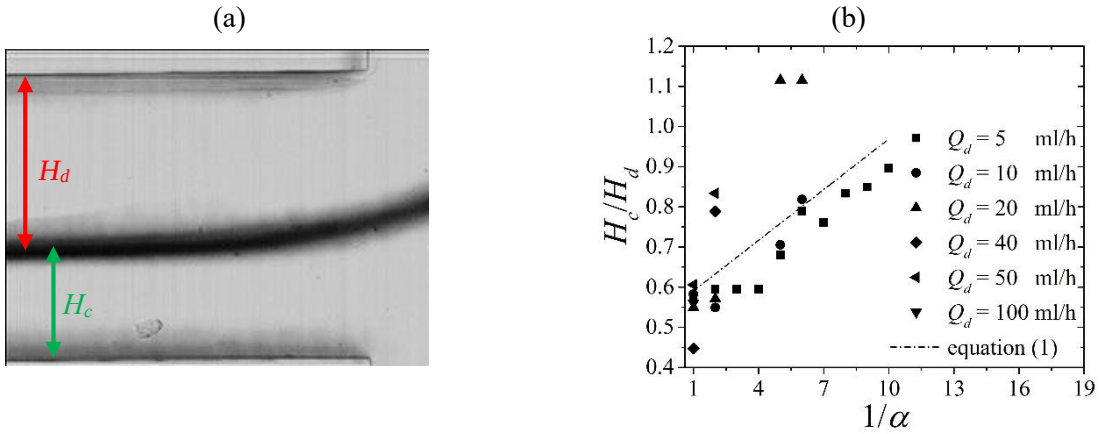

Figure 4. A sketch with H_c and H_d (a) and the trend of the depth ratio H_c/H_d for a stratified flow of water and silicone oil as a function of the flow rate ratio α in an opposite-flow T-junction (b)

The results show that, especially for low oil flow rates (Q_d<10 ml/h), the depth ratio tends to show a linear dependence on the flow rate ratio α. For large oil flow rates all the results tend to collapse to the same value in correspondence of the minimum value of α tested.

The experimental values of H_c/H_d, scale with the correlation:

$$H_c/H_d = 0.549 + (0.042/\alpha) \tag{1}$$

which is represented in figure 4b by means of a dash-dot line. It is interesting to note that the viscosity ratio μ_c/μ_d in this case is equal to 0.0467, approximately similar to the slope of the linear correlation. In this sense, the experimental results suggest that the expression of the correlation can be generalized as follows:

$$H_c/H_d = a + (b/\lambda\alpha) \tag{2}$$

where λ is the viscosity ratio (μ_d/μ_c). In this way the role of the viscosity ratio on the value of the layer depths of the stratified flow is highlighted. About the coefficients a and b introduced in equation (2), they can be seen as a function of the T-junction geometry and the width ratio $\Lambda=w_d/w_c$. More experimental tests with T-junctions having different geometries with different working fluids are needed in order to determine the right value of these coefficients. The depth ratio is strongly influenced by the flow rate of the fluid having lower viscosity (i.e. water in this work); on the contrary, variations of the flow rate linked to the fluid with higher viscosity (i.e. silicone oil) make marginal variations of the depth ratio.

When the flow rate ratio α is increased, the oil droplets start to be generated. For a fixed silicone oil flow rate, a critical value of the water flow rate there exists above which the droplet generation begins. For a fixed oil flow rate of Q_d=5 ml/h the droplet generation starts only when Q_c>80 ml/h; for Q_d=10 ml/h, the droplet generation starts for Q_c>60 ml/h. The critical flow rate ratio in correspondence of which the droplet generation becomes possible seems to have a non-monotonic trend as evidenced by the flow pattern map shown in figure 5. Maybe it is anticipated to see the droplet generation when

Q_c>45 ml/h for Q_d=20 ml/h, but it seems that with the increase in Q_d, the same trend cannot be seen due to the power of the oil flow which does not allow to be pinched by the continuous flow.

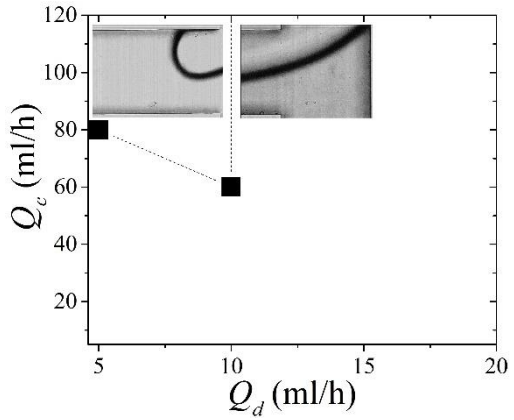

Figure 5. Flow pattern map for water (without surfactant) and silicone oil mixtures as a function of the imposed dispersed (silicone oil) and continuous (water) flow rates

3.3. Water with surfactant

As explained above, the use of Tween 20 added to water changes the flow patterns generated with the T-junction and the droplet formation is greatly enhanced. In this section, all the experimental results have been obtained by adding to water Tween 20 with a concentration equal to 2% in weight.

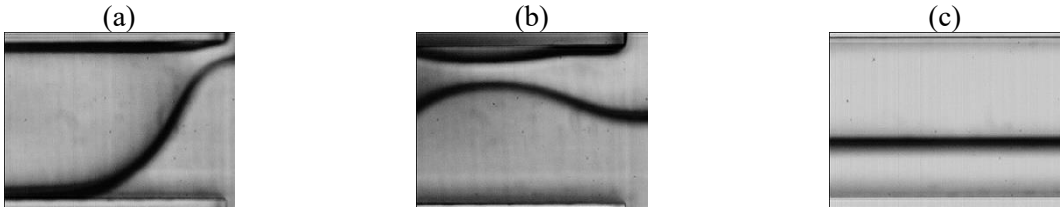

Figure 6. Liquid-liquid interface geometry for different flow regimes: DTJ (a), DC (b) and SF (c)

The water flow rate has varied between 1 to 25 ml/h while the silicone oil flow rate is changed from 0.1 to 13 ml/h. In this case, stratified flow is observed only for very high flow rates of silicone oil. Working with a wide range of flow rates both for dispersed and continuous phase enables the observation of different flow patterns. Three different flow regimes have been identified, namely droplet generation at T-junction (DTJ), downstream of the main channel (DC) and stratified flow (SF). The transition from one flow pattern to another one occurs when the imposed flow rates at the inlets are changed. Figure 7 shows the typical trend of the liquid-liquid interface for the three regimes defined above. In DTJ regime the detachment of the droplet occurs at the edge of the T-junction (see figure 6a), in DC regime the detachment of the droplet occurs downstream (see figure 6b) an in SF regime no droplets are observed (see figure 6c). For low values of α (<2), the droplet generation at the T-junction (DTJ) is mainly due to the squeezing mechanism; the silicone oil is squeezed by water against the edge of the T-junction by generating the detachment of a regular oil droplet. On the contrary, when α is increased the droplet generation occurs downstream of the channel (DC). When the oil flow rate is increased a stratified flow occurs (SF). In figure 7 the three different flow patterns are shown as a function of α and the water flow rate (Q_c). It is clear that in lower water flow rates, the larger values of (α) are needed in order to obtain the passage from one pattern to another one. By increasing α, the detachment point of the droplet moves downstream along the main channel (DC) and the thread formed before detachment increases in size and an elongated filament is observed in the main channel. Stratified flow (SF) is observed only for large values of α.

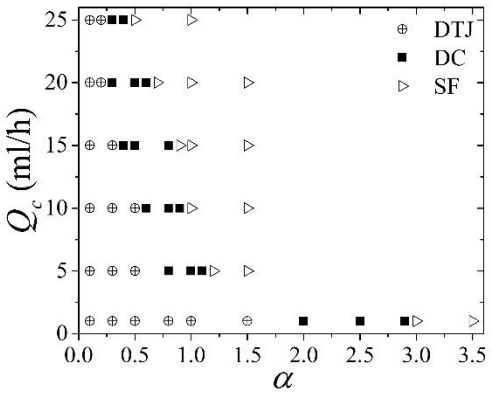

Figure 7. Flow pattern map for a T-junction in opposite-flow configuration as a function of flow rate ratio α (silicone oil-water with a concentration of 2 wt% of Tween 20)

The non-dimensional length of the generated droplets, defined as the ratio between the droplet axial length and the channel width ($\bar{L}=L/w$), is shown in figure 8 as a function of α for both DTJ and DC regimes. The dimensionless length of the droplets tends to increase when α increases. Figure 8 confirms that an increase in Q_c or a decrease in Q_d will produce smaller droplets both in DTJ and DC regimes. When Q_c is increased, the droplets are pinched off earlier and the plug size is reduced. On the other hand, in DTJ regime, an increase in α will result in longer droplets; the experimental data seem to put in evidence that the droplet volume is influenced by the imposed flow rates of both fluids and not only by α [10, 20, 22].

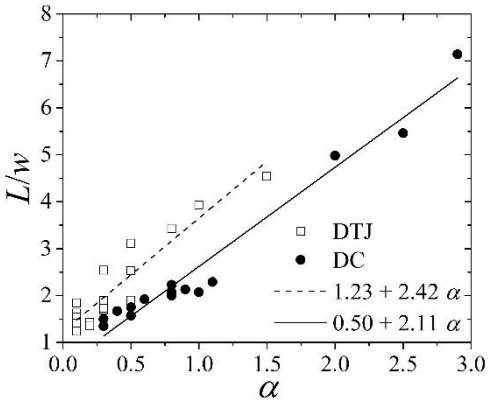

Figure 8. Non-dimensional length of the droplets as a function of flow rate ratio α for different continuous flow rates (empty symbols: DTJ regime; full symbols DC regime)

The increase in α (by increasing Q_d) does not affect the droplet volume significantly; this result indicates that the dispersed flow rate influences the droplet volume through the formation time and it becomes important when low continuous flow rates are imposed at the inlet of the junction. The breakup mechanism in DC regime is similar to the mechanism responsible of the droplet formation in DTJ regime but in DC regime the outlet channel is never completely blocked and the shear force plays a more important role in droplet detachment. By increasing α, the shear force becomes the most important force which governs the fluid flow.

The typical values of polydispersity, defined as the standard deviation of the droplet size distribution divided by the mean droplet size, are reported in table 1. NA means that no experimental test has been carried out under these conditions. For low Q_c, highly monodispersed droplets are generated especially in DTJ regime; it can be observed that the typical values of polydispersity are very low. On the contrary, polydispersity increases in DC regime and very different droplets in size may be obtained especially before the transition from DC to SF regime. Generally, by increasing Q_c

and/or α, the polydispersity increases. $\bar{L}$ obtained in DTJ regime as a function of α shows a linear trend of the data in agreement with the relationship proposed by many authors [22] for squeezing ($\bar{L}=\varepsilon+\omega\alpha$) where ε and ω are two fitting constants which depend on the channel geometry [10].

Table 1. The polydispersity of $\bar{L}$ as a function of the imposed values of α and Q_c (Q_c in ml/h)

	Q_c					
	1	5	10	15	20	25
α						
0.1	0.0233	0.0128	0.0199	0.0121	0.0204	0.0245
0.2	NA	NA	NA	NA	0.0177	0.0230
0.3	0.0258	0.0093	0.0124	0.0097	0.0160	0.0444
0.4	NA	NA	NA	NA	NA	**0.1164**
0.5	0.0308	0.0239	0.0112	0.0209	0.0383	NA
0.6	NA	NA	NA	NA	**0.0972**	NA
0.7	NA	NA	NA	NA	NA	NA
0.8	0.0389	0.0215	0.0249	**0.1416**	NA	NA
0.9	NA	NA	0.0354	NA	NA	NA
1.0	0.0466	0.0246	NA	NA	NA	NA
1.1	NA	0.0244	NA	NA	NA	NA
1.5	0.0706	NA	NA	NA	NA	NA
2.0	**0.1209**	NA	NA	NA	NA	NA
2.5	**0.3638**	NA	NA	NA	NA	NA
2.9	**0.4616**	NA	NA	NA	NA	NA

Figure 9 shows how the fitting coefficients ε and ω have been deducted by using the experimental data; a value of 1.23 for ε and 2.42 for ω has been determined. Similar values have been suggested by other authors for different T-junctions under different flow configurations. The experimental results obey to the squeezing law but it seems that both flow rates (continuous and dispersed) and not only the ratio α influence the droplet length. In figure 9 the Y-bar indicates the droplet polydispersity.

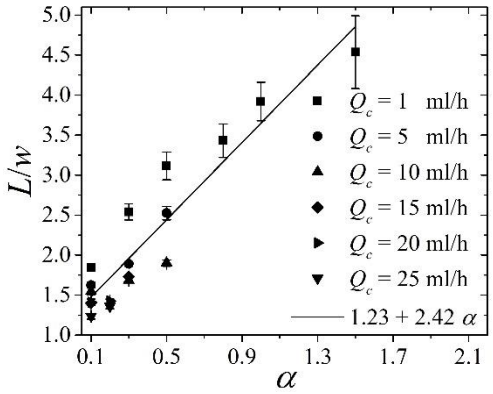

Figure 9. Non-dimensional length of the droplets as a function of α for different continuous flow rates (DTJ regime)

In figure 10 the non-dimensional length of the droplets is given as a function of the imposed continuous flow rate for fixed α. The trend shown in figure 10a is in agreement with previous work [23]; as proposed by Chiarello *et al*. [20], if the droplet non-dimensional length is normalized with $\alpha^{0.25}$ (see figure 10b), the experimental data obtained with different values of α show a more evident

correlation. In addition, from figure 10 it is evident that the cases obtained by imposing a continuous flow rate (Q_c) less than 2 ml/h are characterized by a large value of polydispersity (see also table 1).

These results seem to confirm, as highlighted by other researchers for different flow configurations of the T-junction [10, 20, 22], that $\bar{L}$ in DTJ regime cannot be considered as a function of the flow rate ratio α only but it shows a power-law dependence on the continuous Capillary number, which is proportional to the continuous flow rate.

By considering $\bar{L}$ in DTJ regime both the flow rate ratio and the continuous flow rate and adopting the form of the correlations proposed by Xu *et al*. [10] and Chiarello *et al*. [20], the experimental results obtained in this work by using the T-junction under opposite flow configuration suggest to use β=0.25, in agreement with [20] and m=−0.2 in agreement with [10] for a correlation in form of $k\alpha^{\beta}Q_c^{m}$ while k=4 to obtain a good tuning with the experimental data.

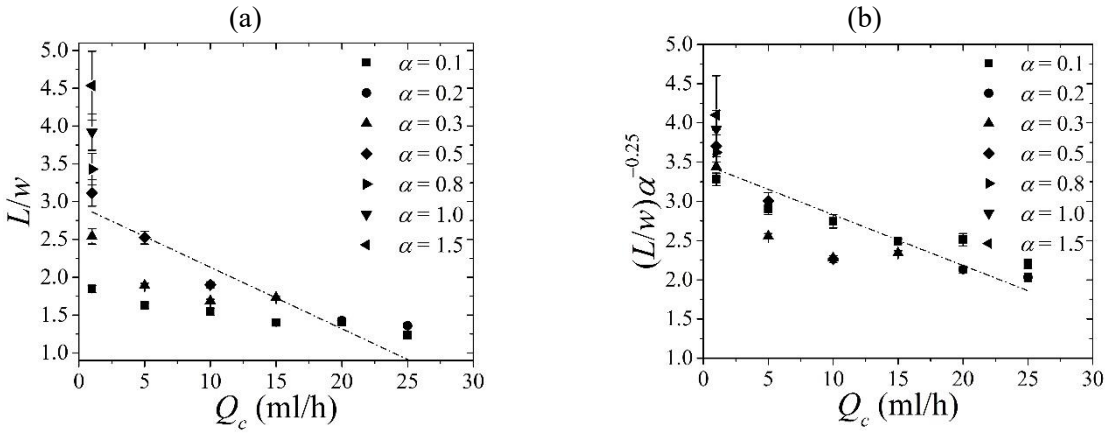

Figure 10. Non-dimensional length (a) and normalized non-dimensional length (b) of the droplets as a function of continuous flow rate for different flow rate ratios for DTJ regime

Figure 11 confirms that, for α<0.5, the power-law dependence of $\bar{L}$ on the continuous Capillary number (flow rate) and α is able to reproduce with an acceptable accuracy the trend of the experimental data obtained in this work.

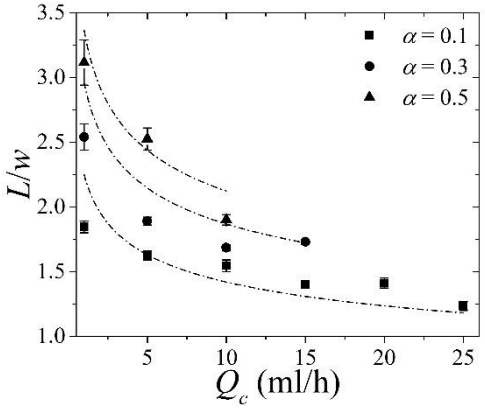

Figure 11. Non-dimensional length of the droplets compared for α<0.5 with the power-law correlation $k\alpha^{\beta}Q_c^{m}$ (DTJ regime)

4. Conclusion

In this work the production of silicone oil-in-water (O/W) droplets within a micro T-junction under opposite-flow configuration is experimentally analyzed. Firstly, the role played by the presence of small concentrations (<2 wt%) of surfactant (Tween 20) in the continuous phase on the droplet

generation has been studied. It has been clearly demonstrated that the use of Tween 20 in water greatly enhances the production of silicone oil plugs; on the contrary, without the use of Tween 20 the main flow regime which can be obtained in a T-junction under opposite flow configuration is the stratified regime when the dispersed flow rate is lower than 100 ml/h and the continuous flow rate is lower than 120 ml/h. In absence of surfactant, an analysis of the depth ratio of water and oil in stratified regime has been made for a wide range of water and silicone oil flow rates; a simple correlation has been proposed in order to predict the value of the depth ratio as a function of the flow rate ratio (α) of the dispersed and the continuous phase. When Tween 20 is added to water three different flow regimes can be detected experimentally, which are namely DTJ (droplet formed at the T-junction), DC (droplet formed at the downstream of the channel) and SF (stratified flow) regimes. The experimental data confirms that the non-dimensional length of the oil plugs depends not only on the flow rate ratio α but also on the continuous Capillary number (flow rate). It has been demonstrated that the correlations proposed by Xu *et al*. [10] and Chiarello *et al*. [20] for the prediction of the non-dimensional length of the plugs still hold for a T-junction under opposite flow configuration.

References

[1] Xiang X, Chen L, Zhuang Q G, Ji X H and He Z K 2012 *Biosens. Bioelectron.* **32** 43-49.
[2] Song H, Chen D L and Ismagilov R F 2006 *Angew. Chem. Int. Edit.* **45** 7336-7356.
[3] Schemberg J, Grodrian A, Romer R, Gastrock G and Lemke K 2009 *Eng. Life. Sci*. **9** 391-397.
[4] Dittrich P S and Manz A 2006 *Nat. Rev. Drug Discov.* **5** 210-218.
[5] Thorsen T, Roberts R W, Arnold F H and Quake S R 2001 *Phys. Rev. Lett*. **86** 4163-4166.
[6] Tice J D, Song H, Lyon A D and Ismagilov R F 2003 *Langmuir* **19** 9127–9133.
[7] Gunther A, Khan S A, Thalmann M, Trachsel F and Jensen K F 2004 *Lab. Chip.* **4** 278–286.
[8] Garstecki P, Fuerstman M J, Stone H A and Whitesides G M 2006 *Lab. Chip.* **6** 437-446.
[9] Steegmans M, Schron C and Boom R 2009 *Chem. Eng. Sci*. **64** 3042-3050.
[10] Xu J, Li S, Tan J and Luo G 2008 *Microfluid. Nanofluid.* **5** 711-717.
[11] Guillot P and Colin A 2005 *Phys. Rev. E.* **72** 066301.
[12] Tan J, Xu J, Li S and Luo G 2008 *Chem. Eng. J.* **136** 306-311.
[13] Das A K and Das P K 2010 *Langmuir* **26** 15883-15894.
[14] Raj R, Mathur N and Buwa V V 2010 *Ind. Eng. Chem. Res*. **49** 10606-10614.
[15] Steegmans M L J , Schroen K and Boom R M 2010b *AICHE J*. **56** 1946-1949.
[16] Yeom S and Lee S Y 2011b *Exp. Therm. Fluid Sci.* **35** 387-394.
[17] Xu J H, Luo G S, Li S W and Chen G G 2006c *Lab. Chip.* **6** 131-136.
[18] Qian D and Lawal A 2006 *Chem. Eng. Sci*. **61** 7609-7625.
[19] Shui L L, van den Berg A and Eijkel J C T 2009 *Lab. Chip*. **9** 795-801.
[20] Chiarello E, Derzsi L, Pierno M, Mistura G and Piccin E 2015 *Micromachines*. **6** 1825-1835.
[21] Pulvirenti B, Rostami B, Puccetti G and Morini G L 2015 *J. Phys.*: *Conf. Ser.* **655** 012028.
[22] Liu H and Zhang Y 2011 *Phys. Fluids*. **23** 082101.
[23] Christopher G F, Noharuddin N N, Taylor J A and Anna S L 2008 *Phys. Rev. E.* **78** 036317.